

# SocialFormer: Social Interaction Modeling with Edge-enhanced Heterogeneous Graph Transformers for Trajectory Prediction

Zixu Wang<sup>1,2\*</sup>, Zhigang Sun<sup>3</sup>, Juergen Luettn<sup>1</sup>, Lavdim Halilaj<sup>1</sup>

**Abstract**—Accurate trajectory prediction is crucial for ensuring safe and efficient autonomous driving. However, most existing methods overlook complex interactions between traffic participants that often govern their future trajectories. In this paper, we propose SocialFormer, an agent interaction-aware trajectory prediction method that leverages the semantic relationship between the target vehicle and surrounding vehicles by making use of the road topology. We also introduce an edge-enhanced heterogeneous graph transformer (EHGT) as the aggregator in a graph neural network (GNN) to encode the semantic and spatial agent interaction information. Additionally, we introduce a temporal encoder based on gated recurrent units (GRU) to model the temporal social behavior of agent movements. Finally, we present an information fusion framework that integrates agent encoding, lane encoding, and agent interaction encoding for a holistic representation of the traffic scene. We evaluate SocialFormer for the trajectory prediction task on the popular nuScenes benchmark and achieve state-of-the-art performance.

## I. INTRODUCTION

Accurately predicting the future trajectory of nearby vehicles is crucial for ensuring the safety of autonomous driving. To achieve this goal, it is important to consider all important factors that govern the future trajectory of a traffic participant. These factors include the road map and topology, agent dynamics, as well as agent interactions [1]. Maps contain important information, including lane boundaries, and possible routes to drive for a given vehicle. Agent dynamics provides information about agents' past movements and direction and may indicate possible future movements. Interactions between agents include the type of maneuver such as lane change, lane keeping, car following, yielding, and giving right-of-way. Furthermore, there exist intricate interactions among agents, where communication plays a role in anticipating the behavior of other agents. Examples include inquiries such as: "Will the agent behind slow down to let me change the lane?" or "Will the vehicle stop at the pedestrian crossing to let me cross the lane?" or "Will the agent stop before the traffic light turns red?". In order to model such intricate social agent interactions, it is important to consider the agents movements and understand their relationship [2]–[7]. Unfortunately, most methods in trajectory prediction are not able to consider such information.

<sup>1</sup>Zixu Wang, Juergen Luettn, and Lavdim Halilaj are with Robert Bosch GmbH {firstname.lastname}@bosch.com

<sup>2</sup>Zixu Wang is with Technical University of Munich {firstname.lastname}@tum.de

<sup>3</sup>Zhigang Sun is with Bosch Center for Artificial Intelligence zhigang.sun3@cn.bosch.com

\* Work done during an internship at Robert Bosch GmbH

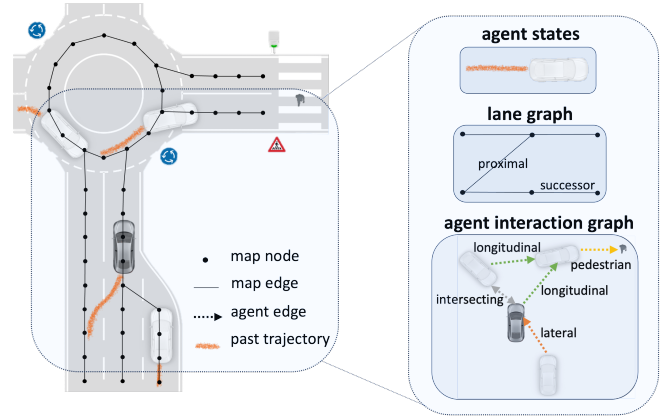


Fig. 1. Schematic illustration of the traffic scene. The future trajectory of a vehicle depends on many factors, including agent states, road topology with possible driving directions and lane changes, and the influence of nearby vehicles. The latter includes past trajectory, relation type, distance, speed, and right of way, among others.

Several methods [8]–[14] consider road maps and agent dynamics, yet they do not account for the representation of social interactions among agents. While certain approaches [15], [16] and [12], [17], [18] adopt homogeneous and heterogeneous graphs, respectively, to model interactions, they often neglect semantic relationships between agents. The manner in which one vehicle influences the trajectory of another is closely tied to their semantic relation within the road network, such as whether a vehicle is ahead of the ego vehicle (*longitudinal*), on an adjacent lane (*lateral*), or on intersecting lanes (*intersecting*). Although recent work [19] incorporates such information, it lacks a complete representation and does not consider all relevant information of the map.

To tackle these challenges, we propose SocialFormer, a novel approach to trajectory prediction that takes into account social agent interactions, leveraging semantic relationships between agents. To model these interactions, we introduce the edge-enhanced heterogeneous graph transformer (EHGT), which extends the capabilities of the heterogeneous graph transformer (HGT) by addressing its deficiency in incorporating edge attributes. EHGT is capable of encoding both the type and attributes of relationships in heterogeneous graphs, effectively representing the traffic scene and agents. Temporal behavior is modeled using GRUs, and we introduce a fusion module that integrates encodings of the target agent, surrounding agents, their interactions, and lane information. Finally, a multi-layer perceptron (MLP) is employed to predict multiple trajectories for the target vehicle. In summary, our main contributions are:

- A novel trajectory prediction architecture that leverages the intricate semantic, spatial, and temporal relationships among agents. This architecture comprises an interaction-aware dynamic heterogeneous graph encoder incorporating interactions between agents with temporal modeling. Additionally, a fusion module is employed to combine various encodings, establishing a comprehensive understanding of the traffic scene for the decoder.
- A novel edge-enhanced heterogeneous graph transformer (EHGT) operator, capable of encoding edge attributes of heterogeneous graphs.
- We demonstrate the effectiveness of our approach on the widely-used nuScenes benchmark and conduct several ablation studies to validate our method’s performance.

## II. RELATED WORK

### A. Raster-based Scene Representation

Raster-based approaches commonly utilize Birds-Eye View (BEV) images as a representation for the map, agents, and related information [8], [20]. Approaches such as [21], [22] encode diverse information into a spatial grid, encompassing the history of static and dynamic entities as well as semantic map details. MultiPath [9] employs a deep structure comprising 15 input channels of information, effectively encapsulating both the static and dynamic aspects of the scene. However, the rasterization process invariably leads to information loss, including geometric and temporal details.

### B. Graph-based Scene Representation

Graph-based methods offer the advantage of explicit modeling of scene entities and their interactions within driving scenarios [23], potentially leading to improved performance in trajectory prediction. Approaches like VectorNet [12] and its extensions [17], [24]–[26] use a hierarchical graph to represent the traffic scene. Additionally, these methods incorporate vectorized scene context information extracted from high-definition (HD) maps to enrich their representations. Compared to VectorNet, the lane graph in LaneGCN [13] and FRM [27] is only sparsely connected. While graph-based representations provide more explicit modeling, these methods mainly rely on homogeneous graphs, limiting their capacity to represent the semantic content of the traffic scene.

### C. Heterogeneous Graph-based Representation

Several approaches try to model different maps and agents with heterogeneous graphs. HEAT [18] extends Graph Attention Networks (GAT) [28] to deal with both heterogeneity and edge features for interaction modeling. In this method, edge type and edge attributes are concatenated as edge features. Subsequently, this edge feature is concatenated with the source node feature to generate a new node feature used for calculating the attention coefficient and subsequent aggregation. Grimm *et al.* [29] use a holistic graph-based method combining time variant information in a single graph, instead of using separate information for each time-step like [30], [31]. This approach is among the first to model the entire encoding step in a single graph for trajectory prediction.

TABLE I  
COMPARISON OF DIFFERENT TRAJECTORY PREDICTION METHODS

| Method             | Data representation                  |                            |                  |                  |                 | Learning approaches |                  |                   |
|--------------------|--------------------------------------|----------------------------|------------------|------------------|-----------------|---------------------|------------------|-------------------|
|                    | Map                                  | Agent                      | A-A <sup>0</sup> |                  |                 | Map                 | Agent            | A-A <sup>0</sup>  |
|                    |                                      |                            | Form             | Rel <sup>1</sup> | EA <sup>2</sup> |                     |                  |                   |
| MTP [8]            | Image                                | Image Vector               | -                | -                | -               | CNN                 | CNN              | CNN               |
| Multipath [9]      | Image                                | Image                      | Image            | -                | -               | CNN                 | CNN              | CNN               |
| ReCoG [10]         | Image                                | Vector                     | HeE <sup>4</sup> | -                | -               | CNN                 | RNN              | GNN               |
| AgentFormer [11]   | Image                                | Vector                     | -                | -                | -               | CNN                 | AF <sup>9</sup>  | AF <sup>9</sup>   |
| VectorNet [12]     | HeN <sup>5</sup>                     | HoN <sup>3</sup>           | -                | -                | -               | MLP                 | MLP              | GNN               |
| LaneGCN [13]       | HoN <sup>3</sup><br>HeE <sup>6</sup> | Vector                     | -                | -                | -               | GNN                 | CNN              | ATT <sup>8</sup>  |
| PGP [14]           | HoN <sup>3</sup>                     | Vector                     | -                | -                | -               | GRU                 | GRU              | -                 |
| HDGT [7]           | HoN <sup>3</sup>                     | HeN <sup>5</sup>           | HeE <sup>6</sup> | -                | ✓               | GT <sup>10</sup>    | GT <sup>10</sup> | GT <sup>10</sup>  |
| GRIP [15]          | -                                    | HoN <sup>3</sup>           | HeE <sup>4</sup> | -                | -               | GCN                 | GCN              | -                 |
| HEAT [18]          | Image                                | HeN <sup>5</sup>           | HeE <sup>6</sup> | -                | ✓               | CNN                 | HEAT             | HEAT              |
| Relation [19]      | NA                                   | HoN <sup>3</sup>           | HeE <sup>6</sup> | ✓                | ✓               | NA                  | GNN              | GNN               |
| LAformer [26]      | Vector                               | Vector                     | -                | -                | -               | ATT <sup>8</sup>    | ATT <sup>8</sup> | -                 |
| FRM [27]           | HoN <sup>3</sup><br>HeE <sup>6</sup> | Vector                     | -                | -                | -               | GNN                 | MLP              | FRM <sup>11</sup> |
| HoliGraph [29]     | HoN <sup>3</sup><br>HeE <sup>6</sup> | HoN <sup>3</sup>           | HeE <sup>6</sup> | ✓                | ✓               | GNN                 | GNN              | GNN               |
| SocialFormer(Ours) | HoN <sup>3</sup><br>HeE <sup>6</sup> | HeE <sup>6</sup><br>Vector | HeE <sup>6</sup> | ✓                | ✓               | GNN                 | GNN              | EHGT              |

<sup>0</sup>A-A: Agent-Agent, <sup>1</sup>Rel: Relation type, <sup>2</sup>EA: Edge Attribute, <sup>3</sup>HoN: Homogeneous Node, <sup>4</sup>HeE: Heterogeneous Edge, <sup>5</sup>HeN: Heterogeneous Node, <sup>6</sup>HeE: Heterogeneous Edge, <sup>7</sup>FPN: Feature Pyramid Network, <sup>8</sup>ATT: Attention, <sup>9</sup>AF: AgentFormer, <sup>10</sup>GT: Graph Transformer, <sup>11</sup>FRM: Future Relationship Module, <sup>12</sup>-: Not modelled, ✓: Modelled

However, the number of GNN layers must correspond to the need for passing information from the first to the last agent node of the trajectory, which will potentially cause an over-smoothing problem.

### D. Agent Interaction Modeling

Several methods have been proposed for modeling the interaction between agents. TNT [17] utilizes a hierarchical heterogeneous graph to represent interactions. Initially, each object is represented by a sub-graph, which is then combined into a fully connected graph. However, learning interactions from such a fully connected graph can be challenging. AgentFormer [11] models interactions between agents in time and interactive dimensions with a transformer mechanism. However, this method also does not directly represent relationships between agents. GRIP [15] explicitly represents interactions between agents using a graph-based approach, where agents close to each other are connected by edges. However, it does not consider edge features such as distance and speed difference. SCALE-Net [16] employs an edge-featured homogeneous graph to represent agent interactions, encoding the relative states between connected agents. HEAT [18] represents interactions as an edge-featured heterogeneous graph but still ignores the semantic relationships among the agents. In [29], Grimm *et al.* uses the edge type *attent* to represent the interaction between agents. In [19], [32], semantic information regarding agent interaction is represented by relation types *longitudinal*, *lateral*, and *intersecting*, ignoring relation with pedestrian. However, these approaches still do not comprehensively represent social interactions.

As shown in Table I, which offers a detailed comparison of different trajectory prediction methods with a particular focus on social interaction modeling between agents, many methods either ignore agent social interaction or only use

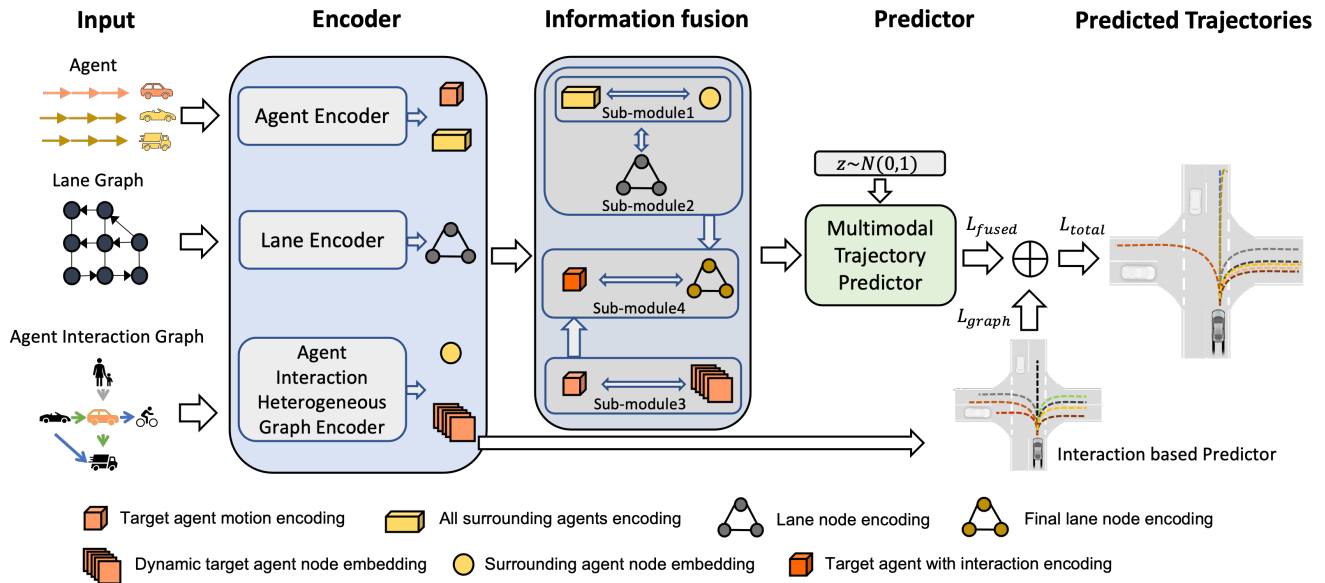


Fig. 2. Overview of proposed SocialFormer. Agent states, lane graphs, and the interactions between agents in the form of heterogeneous graphs are encoded by the specific encoder. An information fusion module is used to generate the holistic latent representation of the traffic scene. Finally, the predictor outputs possible future trajectories of the target agent.

limited information. This omission hinders capturing the insight from the complex traffic scenarios between traffic participants. In this paper, we proposed SocialFormer, a novel approach with a focus on agent social interaction with heterogeneous graphs to address these shortcomings. Incorporating this information from complex traffic scenarios, our architecture is able to learn and then predict trajectories considering the interactive intention of traffic participants.

### III. METHODOLOGY

We first provide an overview of our approach as shown in Fig. 2. Initially, we encode all agent information and lane graphs into latent embeddings. Subsequently, we employ a dynamic heterogeneous graph encoder to encode the agent interaction graph. The information fusion module then integrates the diverse encodings with four sub-modules, forming a holistic representation. Finally, the decoder utilizes the comprehensive representation to predict multi-modal trajectories.

#### A. Lane Graph Representation

We adopt a graph representation for the map in line with [14]. Center lines of lanes are represented as a directed graph, denoted as  $G = \{V, E\}$ . Each node  $v$  denotes a sequence of pose vectors

$$f_{1:N}^v = [f_1^v, f_2^v, \dots, f_N^v], \quad (1)$$

where every pose is characterized by:

$$f_n^v = [x_n^v, y_n^v, \theta_n^v, \underset{\text{stopline crosswalk}}{flag_n^v}, flag_n^v], \quad (2)$$

where  $x_n^v, y_n^v$  are the local coordinates for the  $n$ -th pose and  $\theta_n^v$  is its yaw angle.  $flag$  indicates whether the pose lies on a stop line or crosswalk.

Regarding node inter-relationships, there are two edge types: *successors* and *proximal*. The *successors* edge ensures continuity to the next node along a lane, maintaining a legitimate trajectory. In contrast, the *proximal* edge represents legal lane changes between neighboring lanes traveling in the same direction (see Fig. 1).

#### B. Agent Representation

Agents, categorized as either human or vehicle, are represented as sequences of temporal vectors:

$$f_n^T = [f_n^{t=-4}, f_n^{t=-3}, \dots, f_n^{t=0}], \quad (3)$$

where  $n$  specifies the individual agent. The index  $t$  spans from the earliest observable frame to the present scene (2-second historical states with a 2 Hz sampling rate). Each temporal vector  $f_n^t$  represents state features as

$$f_n^t = [x^t, y^t, vel^t, acc^t, yawrate^t], \quad (4)$$

indicating the location, velocity, acceleration, and yaw rate of  $n$ -th agent at  $t$ .

#### C. Lane and Agent Encoder

In order to model the temporal dynamics of the agents, we first use an MLP followed by GRUs to encode lane node features  $f_{1:N}^v$ , target agent's states  $f_{target}^T$  and surrounding agent's states  $f_{surr}^T$ . The output from each GRU serves as the embedding for the lane node ( $h_{lane}$ ), the target agent ( $h_{target}$ ), and surrounding agents ( $h_{surr}$ ).

#### D. Agent Interaction Representation

When driving, humans rely on a complex interplay of factors to prioritize which surrounding vehicles or agents are most relevant. Based on the work

of [33] and [34], we identify the inter-agent relationships by four distinct edge types: *Longitudinal*, *Intersecting*, *Lateral*, and *Pedestrian* with three edge attributes  $f_{edge}^{(s,t)} = [Distance, PathDistance, EdgeProbability]$  (see Fig. 1), where *Distance* quantifies the Euclidean distance, *PathDistance* specifies the distance traversed along a specific path, and *EdgeProbability* provides the likelihood of a particular relation. Notably, the *Pedestrian* edge type does not possess the *PathDistance* attribute.

### E. Agent Interaction Dynamic Encoding

To model the different dynamic behavioral patterns of different agent types (e.g., vehicle or pedestrian), we use distinct MLPs as specific type encoder to encode them, as shown in Fig. 3. Subsequently, we leverage an EHGT to encode 2-second historical and current agent interaction graphs. Finally, a temporal encoder is deployed to capture temporal changes in the agent interactions.

While Heterogeneous Graph Transformer (HGT) [35] has proven effective in modeling relational data within heterogeneous graphs, its inability to incorporate edge attributes constrains its application in scenarios where the crucial information conveyed by attributes associated with the edges is required. To tackle this problem, we propose EHGT, an extension of HGT, which is able to incorporate edge attributes into the mutual attention and message-passing stages, offering a more comprehensive graph representation. In mutual attention, target node  $t$  is projected into a Query vector, while the source node  $s$  is mapped into a Key vector:

$$Q_{(t)}^i = Q\_Linear_{\tau(t)}^i(H^{l-1}[t]) \quad (5)$$

$$K_{(s)}^i = K\_Linear_{\tau(s)}^i(H^{l-1}[s]), \quad (6)$$

where  $H^{(l-1)}$  is the input from the previous layer and  $i$  refers to the specific attention head. Each node type has a unique linear projection. When computing the attention head, we employ an edge attribute matrix  $W_{\phi(e)}^{Eg\_Attr}$ :

$$ATT\_head^i(s, e, t) = (K_{(s)}^i W_{\phi(e)}^{ATT} W_{\phi(e)}^{Eg\_Attr} Q_{(t)}^i)^T \cdot \frac{\mu_{\langle \tau(s), \phi(e), \tau(t) \rangle}}{\sqrt{d}}, \quad (7)$$

where  $W_{\phi(e)}^{ATT}$  is a matrix specific to the edge type, designed to capture the semantic relations  $\phi(e)$  between nodes. Furthermore,  $\mu$  stands as an adaptive parameter, signifying the importance of each relation triple  $\langle source\ node, edge, target\ node \rangle$ , while  $d$  represents the dimensionality of the vector. Then  $h$  attention heads are concatenated, and the *Softmax* function is applied to determine the final attention weights for each relation triple:

$$ATT_{EHGT}(s, e, t) = \underset{s \in N(t)}{Softmax}(\|_{i \in [1, h]} ATT\_head^i(s, e, t)). \quad (8)$$

The message-passing runs in parallel with the mutual attention computation. To compute  $i$ -th message head  $MSG\_head^i(s, e, t)$ , the representation of the source node from the preceding layer  $H^{l-1}[s]$  is projected by a node type encoder  $M\_Linear$ . Subsequently, it is multiplied by the edge

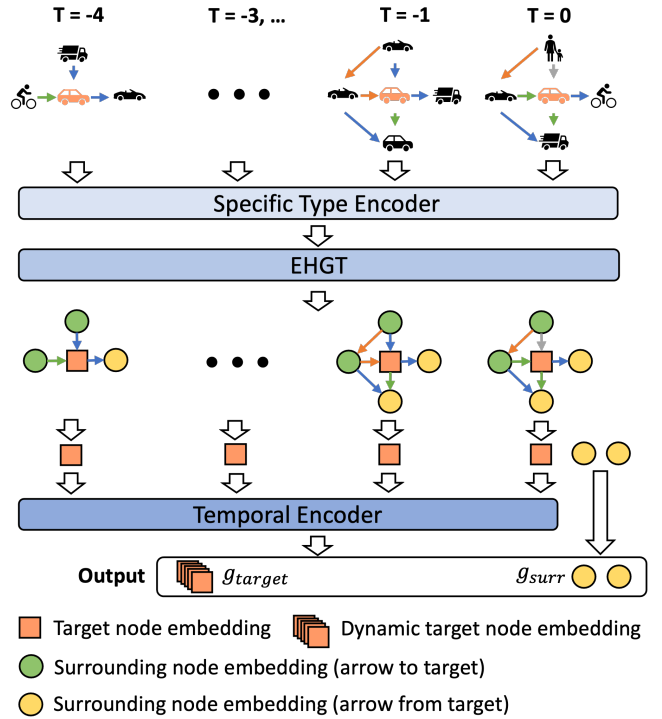


Fig. 3. Illustration of Agent Interaction Dynamic Heterogeneous Graph Encoder: It consists of three parts: specific type encoder, EHGT, and temporal encoder.

attribute matrix  $W_{\phi(e)}^{Eg\_Attr}$  and matrix  $W_{\phi(e)}^{MSG}$  to integrate the edge dependency:

$$MSG\_head^i(s, e, t) = M\_Linear_{\tau(s)}^i(H^{l-1}[s]) W_{\phi(e)}^{Eg\_Attr} W_{\phi(e)}^{MSG}. \quad (9)$$

We then concatenate  $h$  message nodes for each node pair to obtain  $MSG_{EHGT}(s, e, t)$ :

$$MSG_{EHGT}(s, e, t) = \|_{i \in [1, h]} MSG\_head^i(s, e, t). \quad (10)$$

In the subsequent aggregation phase, messages from all source nodes  $s$  are aggregated to the target node  $t$ . The attention vector in Eq. 8 serves as the weight to average the corresponding messages from source nodes in Eq. 10. This results in the updated  $\tilde{H}^{(l)}[t]$ :

$$\tilde{H}^{(l)}[t] = \oplus_{s \in N(t)} (ATT_{EHGT}(s, e, t) \cdot MSG_{EHGT}(s, e, t)). \quad (11)$$

After this,  $\tilde{H}^{(l)}[t]$  contains comprehensive information from the target node  $t$ 's neighbors and their associated relations. The target node  $t$  is then remapped to its type-specific distribution and augmented with a residual connection from the previous layer:

$$H^{(l)}[t] = A\_Linear_{\tau(t)}(\sigma(\tilde{H}^{(l)}[t])) + H^{(l-1)}[t]. \quad (12)$$

EHGT enables the processing of heterogeneous graphs with edge attributes. We employ EHGT to process agent interaction heterogeneous graphs. In practical scenarios, it is typically only the direct neighbor of a target vehicle that significantly influences its behavior. Therefore, we restrict our aggregation for surrounding agents within one hop.

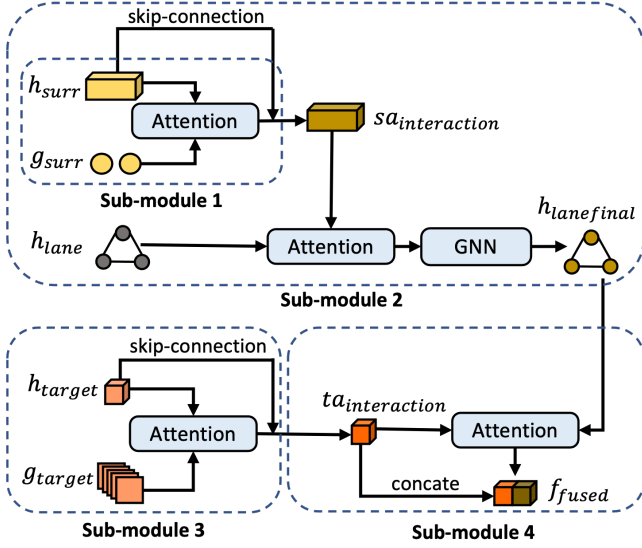


Fig. 4. Information Fusion Module: Four sub-modules combine different encodings to form a comprehensive encoding for the predictor. The output is  $f_{fused}$ .

To capture the evolution of traffic scenes over time, we employ a temporal encoder with GRU, which encodes the target node embeddings sourced from all observed traffic scenes in temporal order, resulting in a dynamic target node graph embedding  $g_{target}$ . Simultaneously, we preserve the embedding of surrounding nodes  $g_{surr}$  from the last observed traffic scene (see Fig. 3), specifically, those nodes that emanate arrows from the target agent, to ensure that we do not lose sight of potential agents affecting prediction.

#### F. Information Fusion

As described above, several encodings are utilized to comprehensively represent the dynamic and interactive information within traffic scenes:

- Target Agent Motion Encoding ( $h_{target}$ ): This captures the movements of the target agent.
- Surrounding Agents Encoding ( $h_{surr}$ ): This encoding provides information about all non-target agents within a traffic scene.
- Lane Node Encoding ( $h_{lane}$ ): This gives insights into the structured lanes in the scene.
- Dynamic Target Node Graph Embedding ( $g_{target}$ ): This embedding represents the target agent’s interactions and relations within a dynamic graph.
- Surrounding Agent Interactive Embedding ( $g_{surr}$ ): This captures how the surrounding agents interact with each other and with the target agent.

To optimally integrate the insights from these encodings, we employ an information fusion module with four sub-modules, as shown in Fig. 4.

1) *Sub-module 1: Surrounding Agents and their Interactions*: To extract meaningful representations that highlight the most influential surrounding agents and understand the significance of their interactions, we deploy a cross-attention

mechanism to weigh and understand which relationships of the surrounding agents are most relevant in the given context. The output of the Sub-module 1  $sa_{interaction}$  denotes the surrounding agents with their encoded interactions:

$$sa_{interaction} = CrossAttention(h_{surr}, g_{surr}) + h_{surr}. \quad (13)$$

Besides, we add a skip-connection to ensure the transfer of the original information across the cross-attention layers and to stabilize the model, especially when the interaction graph is sparse.

2) *Sub-module 2: Surrounding Agents with Interaction and Lane Information*: Incorporating a cross-attention mechanism between  $sa_{interaction}$  and  $h_{lane}$  ensures that the lane node embeddings are refined based on the presence and behavior of agents close to them. We then use GNN to update lane node embedding with other connected lane nodes. After this, we have the final encoding  $h_{lane_{final}}$  for lane information, which is both context-aware (in terms of agent interactive behaviors) and structurally informed (in terms of lane configurations):

$$h_{lane_{final}} = GNN(CrossAttention(h_{lane}, sa_{interaction})). \quad (14)$$

3) *Sub-module 3: Target Agent and its dynamic Interaction*: Similar to Sub-module 1, we like the target agent to be aware of the broader context in which it operates, especially considering its interactions with nearby agents. We therefore refine  $h_{target}$  by fusing it with  $g_{target}$ :

$$ta_{interaction} = CrossAttention(h_{target}, g_{target}) + h_{target}, \quad (15)$$

where  $ta_{interaction}$  indicates the target agent with interaction encoding that is richly informed by its inherent attributes and social interactions with other agents.

4) *Sub-module 4: Target Agent with Interaction Encoding and Lane Final Encoding*: We apply the attention mechanism to weigh the relevance of various features from  $h_{lane_{final}}$  to  $ta_{interaction}$ :

$$f_{fused} = Concatenate(ta_{interaction}, CrossAtt(ta_{interaction}, h_{lane_{final}})). \quad (16)$$

Intuitively, this allows our module to focus on the most pertinent lane-related information while considering a target agent’s interaction. Then, we concatenate  $ta_{interaction}$  with the attention output to ensure that it not only captures the weighted information from the lanes but also preserves the raw interaction details of the target agents. Finally, we obtain the holistic fused encoding  $f_{fused}$ , which is the final encoding of the information fusion module.

This step is crucial as it is the final information fusion process. It provides a complete encoding that includes the specific details from the target agent’s view and its interactions with others and the lanes around it.

#### G. Multimodal Trajectory Predictor

The fused information is then processed by the multimodal trajectory predictor. We concatenate the Gaussian distribution variable  $z$  with the fused encoding  $f_{fused}$ , so that the decoder is equipped to generate diverse motion profiles,

accounting for the inherent uncertainty. Then we use a MLP to output  $k$  mode future trajectories  $\hat{Y}_{1:t_f}^k$ :

$$\hat{Y}_{1:t_f}^k = \text{MLP}(\text{concate}(f_{fused}, z_k)). \quad (17)$$

We then adopt K-means clustering and output the cluster centers as the final output of  $K$  predictions  $[\hat{Y}_{1:t_f}^1, \hat{Y}_{1:t_f}^2, \dots, \hat{Y}_{1:t_f}^k]$ . Besides, we also decode the dynamic target node graph embedding  $g_{target}$  directly to trajectories  $\tilde{Y}_{1:t_f}^k$ . Based on these two outputs, we train our decoder with winner-takes-all average displacement error. In this way, we have two losses: fused regression loss  $\mathcal{L}_{fr}$  and graph regression loss  $\mathcal{L}_{gr}$  and a combined loss of them:

$$\mathcal{L} = \lambda_1 \mathcal{L}_{fr} + \lambda_2 \mathcal{L}_{gr}. \quad (18)$$

with

$$\mathcal{L}_{fr} = \min_k \frac{1}{t_f} \sum_{t=1}^{t_f} \left\| \hat{Y}_t^k - Y_t^{gt} \right\|_2, \quad (19)$$

$$\mathcal{L}_{gr} = \min_k \frac{1}{t_f} \sum_{t=1}^{t_f} \left\| \tilde{Y}_t^k - Y_t^{gt} \right\|_2. \quad (20)$$

The combined loss  $\mathcal{L}$  brings together the strengths of both individual losses, pushing the model to learn from the rich spatial, semantic, and temporal features embedded in  $\mathcal{L}_{fr}$  and  $\mathcal{L}_{gr}$ , ensuring a comprehensive learning process.

#### IV. EXPERIMENT

We evaluate our proposed SocialFormer for the nuScenes prediction challenge, which is to predict the 6-second future trajectory of the target vehicle, given 2-second historical data with a sampling rate of 2Hz. A performance comparison with state-of-the-art approaches and adequate ablation studies are demonstrated.

##### A. Dataset

We use the widely-used public nuScenes dataset [36] and the traffic scene graph dataset nSTP [34], which is a heterogeneous graph dataset representing the nuScenes dataset. It models all scene participants, road elements, and their semantic and spatial relationships. In total, 32186 training samples and 9041 validation samples are utilized for our experiments.

##### B. Metrics

We use Average displacement error (ADE<sub>k</sub>) and miss rate (MR<sub>k</sub>) as evaluation metrics. ADE<sub>k</sub> is to quantify average L2 distance errors between the predicted trajectory and the ground truth (GT), whereas MR<sub>k</sub> denotes the percentage of cases for the maximum L2 distance error is larger than 2 meters over  $k$  most likely predictions.

##### C. Experimental Setup

We implemented and trained our SocialFormer method in the PyTorch framework [37] using the Nvidia V100 GPU server. All graphs are handled with PyTorch Geometric (PyG) [38], a popular library for developing GNNs for structured data applications. We apply the AdamW optimizer [39] with an initial learning rate of 0.001.

TABLE II  
RESULTS ON NUSCENES BENCHMARK FOR DIFFERENT MODELS

| Model               | ADE <sub>5</sub> | MR <sub>5</sub> | ADE <sub>10</sub> | MR <sub>10</sub> |
|---------------------|------------------|-----------------|-------------------|------------------|
| Multipath [9]       | 2.32             | -               | 1.96              | -                |
| CoverNet [40]       | 1.96             | 0.67            | 1.48              | -                |
| P2T [41]            | 1.45             | 0.64            | 1.16              | 0.46             |
| Trajectron++ [42]   | 1.88             | 0.70            | 1.51              | 0.57             |
| AgentFormer [11]    | 1.86             | -               | 1.45              | -                |
| Autobot [43]        | 1.37             | 0.62            | 1.03              | 0.44             |
| SG-Net [44]         | 1.86             | 0.67            | 1.40              | 0.52             |
| PGP [14]            | <b>1.30</b>      | <u>0.61</u>     | <u>1.00</u>       | <b>0.37</b>      |
| HeteGraph [32]      | -                | -               | 1.29              | 0.57             |
| SocialFormer (Ours) | <u>1.32</u>      | <b>0.58</b>     | <b>0.98</b>       | <u>0.39</u>      |

#### V. RESULT

A comparison of the results with SocialFormer and state-of-the-art methods is shown in Table II, which presents the results obtained on the nuScenes validation set. Metrics are the minimum average displacement error ADE and miss rate MR for the top 5 and top 10 predictions, respectively. We highlight the best results in boldface and the second-best results in underlined. Our method achieves the best prediction accuracy for the MR<sub>5</sub> and ADE<sub>10</sub> metrics. For the metrics ADE<sub>5</sub> and MR<sub>10</sub>, our SocialFormer outperforms other state-of-the-art models except PGP [14]. This demonstrates the effectiveness of our SocialFormer in the trajectory prediction task.

It is worth noting that not all traffic scenes exhibit all four defined relation types. Moreover, there are 959 scenes (i.e., 2.33% of all samples) that lack any defined semantic relations, which is because the interactions between two agents do not fit the predefined relation categories, other agents are located more than one lane away from the target agent, or even there are no or very sparse agents surrounding to the target agent. However, our SocialFormer still shows robust performance in predicting the future trajectory of the target agent.

1) *Qualitative Results*: In Fig. 5, we present qualitative results of our model in different scenarios, with each row representing a unique scenario. In scenario ④, our model accurately generates predictions in straightforward driving with longitudinal diversity. Scenario ① illustrates a complex roundabout scene, where our model predicts diverse routes, with most predictions being correct. In scenarios ③, accurate predictions are generated at intersections. Meanwhile, in scenarios ② and ⑤, our model accurately predicts various routes in left-turn situations with a possibility of lane change.

2) *Ablation Study*: We conduct an ablation study to validate the effect of each component in our architecture, including different widely-used GNN operators, temporal encoder, and diverse information fusion strategies. The baseline model predicts trajectories solely based on map and agent data, excluding interactions between agents. In Table III, we compare the performance of both homogeneous (i.e., GAT and GCN) and heterogeneous GNN operators (i.e., heterogeneous graph attention network (HAN) and RGAT).

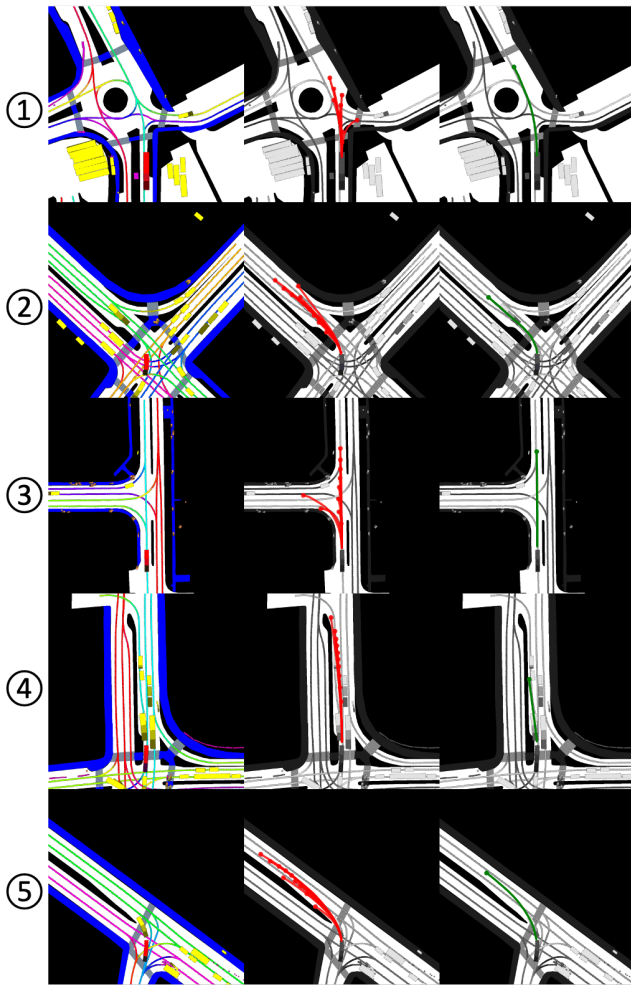


Fig. 5. Illustration of the qualitative result in various traffic scenarios. Left column: HD maps and tracks. Middle column: Top 10 most likely predictions. Right column: Ground truth.

We also explore  $HGT_{\text{concat}}$ , which simply concatenates edge attributes (EA) to node features.

We observe an improvement on all metrics with the integration of edge attributes using our EHGT, underscoring the significance of effectively modeling edge attributes.

TABLE III

ABLATION STUDY ON EDGE ATTRIBUTE AND GNN OPERATORS

| EA | GNN                   | ADE <sub>5</sub> | MR <sub>5</sub> | FDE <sub>5</sub> | ADE <sub>10</sub> | MR <sub>10</sub> | FDE <sub>10</sub> |
|----|-----------------------|------------------|-----------------|------------------|-------------------|------------------|-------------------|
| ×  | HGT                   | 1.35             | <b>0.58</b>     | 2.72             | 0.99              | 0.40             | 1.70              |
| ×  | GAT                   | 1.35             | 0.59            | 2.71             | 0.99              | 0.40             | 1.71              |
| ×  | GCN                   | 1.36             | 0.60            | 2.70             | 0.99              | 0.41             | 1.71              |
| ×  | HAN                   | 1.35             | 0.60            | 2.67             | <b>0.98</b>       | 0.40             | 1.68              |
| ✓  | RGAT                  | 1.36             | 0.60            | 2.68             | 0.99              | <b>0.39</b>      | 1.68              |
| ✓  | $HGT_{\text{concat}}$ | 1.35             | <b>0.58</b>     | 2.67             | 0.99              | <b>0.39</b>      | 1.69              |
| ✓  | EHGT(Ours)            | <b>1.32</b>      | <b>0.58</b>     | <b>2.64</b>      | <b>0.98</b>       | <b>0.39</b>      | <b>1.67</b>       |

Table IV demonstrates a performance improvement with the inclusion of a temporal encoder, which indicates the significance of social interactions in the temporal dimension. However, the skip connections do not yield a substantial benefit. This observation may be attributed to the relatively shallow depth of our model.

TABLE IV

ABLATION STUDY ON FUSION METHODS AND TEMPORAL ENCODER

| Temp. Enc. | Fusion    | ADE <sub>5</sub> | MR <sub>5</sub> | FDE <sub>5</sub> | ADE <sub>10</sub> | MR <sub>10</sub> | FDE <sub>10</sub> |
|------------|-----------|------------------|-----------------|------------------|-------------------|------------------|-------------------|
| ×          | Att.      | 1.35             | <b>0.57</b>     | 2.73             | 0.99              | 0.40             | <b>1.64</b>       |
| ×          | Att.,Skip | 1.35             | 0.58            | 2.72             | 0.99              | 0.40             | <b>1.64</b>       |
| ✓          | Att.      | 1.33             | 0.58            | <b>2.64</b>      | 0.99              | 0.40             | 1.67              |
| ✓          | Att.,Skip | <b>1.32</b>      | 0.58            | <b>2.64</b>      | <b>0.98</b>       | <b>0.39</b>      | 1.67              |

3) *Sensitivity Analysis of the Hyper-Parameters*: We conducted an empirical study by varying the weights of the fused regression loss in Eq. 18. The results in Table V reveal that the combination of  $\lambda_1 = 1$  and  $\lambda_2 = 0.5$  yields the best performance across all metrics. These findings underscore the efficacy of the encoding from the dynamic heterogeneous graph encoder in enhancing the model’s understanding of agent interaction graphs. Acting as part of the auxiliary task, the graph loss ensures that the loss is effectively propagated into the graph encoder within the intricate architecture.

TABLE V

COMPARISON OF DIFFERENT LOSS WEIGHT COMBINATION

| $\lambda_1$ | $\lambda_2$ | ADE <sub>5</sub> | MR <sub>5</sub> | FDE <sub>5</sub> | ADE <sub>10</sub> | MR <sub>10</sub> | FDE <sub>10</sub> |
|-------------|-------------|------------------|-----------------|------------------|-------------------|------------------|-------------------|
| 1           | 0           | 1.34             | 0.60            | 2.65             | 0.98              | 0.39             | 1.68              |
| 1           | 0.2         | 1.34             | 0.59            | 2.65             | 0.99              | 0.41             | 1.67              |
| <b>1</b>    | <b>0.5</b>  | <b>1.32</b>      | <b>0.58</b>     | <b>2.64</b>      | 0.98              | 0.39             | 1.67              |
| 1           | 1           | 1.36             | 0.61            | 2.66             | 0.99              | 0.41             | 1.69              |

## VI. CONCLUSION

This paper introduced SocialFormer, a novel trajectory prediction architecture that integrates agent interaction with heterogeneous graphs. We proposed the edge-enhanced graph transformer (EHGT) to encode the semantic relations and their attributes and a GRU-based temporal encoder to extract semantic relations in the temporal domain. A fusion module was proposed to integrate the diverse agent, lane, and interaction encodings in a more comprehensive manner. Experiments demonstrate that our model achieves state-of-the-art performance on the popular nuScenes dataset, even when sparse or no semantic information exists in some traffic scenes. It also indicates that social interaction modeling could improve other trajectory prediction methods. Future work will consider employing the information on traffic signs and lights and incorporating anchor paths to remove unrealistic predictions and to avoid mode collapse.

## REFERENCES

- [1] Y. Huang, J. Du, Z. Yang, Z. Zhou, L. Zhang, and H. Chen, “A survey on trajectory-prediction methods for autonomous driving,” *IEEE Transactions on Intelligent Vehicles*, vol. 7, pp. 652–674, 2022.
- [2] Z. Ding and H. Zhao, “Incorporating driving knowledge in deep learning based vehicle trajectory prediction: A survey,” *IEEE Transactions on Intelligent Vehicles*, vol. 8, pp. 3996–4015, 2023.
- [3] Y. Hu, A. Nakhaei, M. Tomizuka, and K. Fujimura, “Interaction-aware decision making with adaptive strategies under merging scenarios,” in *2019 IEEE/RSJ International Conference on Intelligent Robots and Systems (IROS)*. IEEE, 2019, pp. 151–158.
- [4] L. Sur, C. Tang, Y. Niu, E. Sachdeva, C. Choi, T. Misu, M. Tomizuka, and W. Zhan, “Domain knowledge driven pseudo labels for interpretable goal-conditioned interactive trajectory prediction,” in *IEEE/RSJ International Conference on Intelligent Robots and Systems (IROS)*, 2022.

- [5] S. Kumar, Y. Gu, J. Hoang, G. C. Haynes, and M. Marchetti-Bowick, "Interaction-based trajectory prediction over a hybrid traffic graph," in *2021 IEEE/RSJ International Conference on Intelligent Robots and Systems (IROS)*. IEEE, 2021, pp. 5530–5535.
- [6] E. M. Rella, J.-N. Zaech, A. Liniger, and L. Van Gool, "Decoder fusion rnn: Context and interaction aware decoders for trajectory prediction," in *2021 IEEE/RSJ International Conference on Intelligent Robots and Systems (IROS)*. IEEE, 2021, pp. 5937–5943.
- [7] X. Jia, P. Wu, L. Chen, Y. Liu, H. Li, and J. Yan, "Hdgt: Heterogeneous driving graph transformer for multi-agent trajectory prediction via scene encoding," *IEEE transactions on pattern analysis and machine intelligence*, 2023.
- [8] H. Cui, V. Radosavljevic, F.-C. Chou, T.-H. Lin, T. Nguyen, T.-K. Huang, J. Schneider, and N. Djuric, "Multimodal trajectory predictions for autonomous driving using deep convolutional networks," in *Int. Conference on Robotics and Automation (ICRA)*. IEEE, 2019.
- [9] Y. Chai, B. Sapp, M. Bansal, and D. Anguelov, "Multipath: Multiple probabilistic anchor trajectory hypotheses for behavior prediction," in *Conference on Robot Learning*, 2019.
- [10] X. Mo, Y. Xing, and C. Lv, "Recog: A deep learning framework with heterogeneous graph for interaction-aware trajectory prediction," *CoRR*, vol. abs/2012.05032, 2020.
- [11] Y. Yuan, X. Weng, Y. Ou, and K. M. Kitani, "Agentformer: Agent-aware transformers for socio-temporal multi-agent forecasting," in *Proceedings of the IEEE/CVF International Conference on Computer Vision*, 2021, pp. 9813–9823.
- [12] J. Gao, C. Sun, H. Zhao, Y. Shen, D. Anguelov, C. Li, and C. Schmid, "Vectormet: Encoding hd maps and agent dynamics from vectorized representation," in *Proceedings of the IEEE/CVF Conference on Computer Vision and Pattern Recognition*, 2020, pp. 11 525–11 533.
- [13] M. Liang, B. Yang, R. Hu, Y. Chen, R. Liao, S. Feng, and R. Urtasun, "Learning lane graph representations for motion forecasting," in *Computer Vision–ECCV: 16th European Conference, Glasgow, Proceedings, Part II 16*. Springer, 2020.
- [14] N. Deo, E. Wolff, and O. Beijbom, "Multimodal trajectory prediction conditioned on lane-graph traversals," in *Conference on Robot Learning*. PMLR, 2022, pp. 203–212.
- [15] X. Li, X. Ying, and M. C. Chuah, "Grip: Graph-based interaction-aware trajectory prediction," in *2019 IEEE Intelligent Transportation Systems Conference (ITSC)*. IEEE, 2019, pp. 3960–3966.
- [16] H. Jeon, J. Choi, and D. Kum, "Scale-net: Scalable vehicle trajectory prediction network under random number of interacting vehicles via edge-enhanced graph convolutional neural network," in *2020 IEEE/RSJ International Conference on Intelligent Robots and Systems (IROS)*. IEEE, 2020, pp. 2095–2102.
- [17] H. Zhao, J. Gao, T. Lan, C. Sun, B. Sapp, B. Varadarajan, Y. Shen, Y. Shen, Y. Chai, C. Schmid *et al.*, "Tnt: Target-driven trajectory prediction," in *Conference on Robot Learning*. PMLR, 2021, pp. 895–904.
- [18] X. Mo, Z. Huang, Y. Xing, and C. Lv, "Multi-agent trajectory prediction with heterogeneous edge-enhanced graph attention network," *IEEE Transactions on Intelligent Transportation Systems*, vol. 23, no. 7, pp. 9554–9567, 2022.
- [19] M. Zipfl, F. Hertlein, A. Rettinger, S. Thoma, L. Halilaj, J. Luetttin, S. Schmid, and C. Henson, "Relation-based motion prediction using traffic scene graphs," in *25th International Conference on Intelligent Transportation Systems (ITSC)*. IEEE, 2022.
- [20] H. Berkemeyer, R. Franceschini, T. Tran, L. Che, and G. Pipa, "Feasible and adaptive multimodal trajectory prediction with semantic maneuver fusion," in *International Conference on Robotics and Automation (ICRA)*. IEEE, 2021.
- [21] M. Bansal, A. Krizhevsky, and A. Ogale, "Chauffeurnet: Learning to drive by imitating the best and synthesizing the worst," *arXiv preprint arXiv:1812.03079*, 2018.
- [22] J. Hong, B. Sapp, and J. Philbin, "Rules of the road: Predicting driving behavior with a convolutional model of semantic interactions," in *Proceedings of the IEEE/CVF Conference on Computer Vision and Pattern Recognition*, 2019, pp. 8454–8462.
- [23] L. Halilaj, I. Dindorkar, J. Lüttin, and S. Rothermel, "A knowledge graph-based approach for situation comprehension in driving scenarios," in *The Semantic Web: 18th International Conference, ESWC Proceedings*. Springer, 2021.
- [24] J. Gu, C. Sun, and H. Zhao, "Densent: End-to-end trajectory prediction from dense goal sets," in *Proceedings of the IEEE/CVF International Conference on Computer Vision*, 2021.
- [25] Z. Huang, X. Mo, and C. Lv, "Multi-modal motion prediction with transformer-based neural network for autonomous driving," in *Int. Conference on Robotics and Automation (ICRA)*. IEEE, 2022.
- [26] M. Liu, H. Cheng, L. Chen, H. Broszio, J. Li, R. Zhao, M. Sester, and M. Y. Yang, "Laformer: Trajectory prediction for autonomous driving with lane-aware scene constraints," *CoRR*, vol. abs/2302.13933, 2023.
- [27] D. Park, H. Ryu, Y. Yang, J. Cho, J. Kim, and K. Yoon, "Leveraging future relationship reasoning for vehicle trajectory prediction," in *The Eleventh International Conference on Learning Representations, ICLR 2023, Kigali, Rwanda, May 1-5, 2023*. OpenReview.net, 2023.
- [28] P. Veličković, G. Cucurull, A. Casanova, A. Romero, P. Lio, and Y. Bengio, "Graph attention networks," *arXiv preprint arXiv:1710.10903*, 2017.
- [29] D. Grimm, P. Schörner, M. Dreßler, and J.-M. Zöllner, "Holistic graph-based motion prediction," in *International Conference on Robotics and Automation (ICRA)*. IEEE, 2023.
- [30] Z. Sheng, Y. Xu, S. Xue, and D. Li, "Graph-based spatial-temporal convolutional network for vehicle trajectory prediction in autonomous driving," *IEEE Transactions on Intelligent Transportation Systems*, vol. 23, no. 10, pp. 17 654–17 665, 2022.
- [31] D. Cao, J. Li, H. Ma, and M. Tomizuka, "Spectral temporal graph neural network for trajectory prediction," in *International Conference on Robotics and Automation (ICRA)*. IEEE, 2021.
- [32] D. Grimm, M. Zipfl, F. Hertlein, A. Naumann, J. Lüttin, S. Thoma, S. Schmid, L. Halilaj, A. Rettinger, and J. M. Zöllner, "Heterogeneous graph-based trajectory prediction using local map context and social interactions," *2023 IEEE 26th International Conference on Intelligent Transportation Systems (ITSC)*, pp. 2901–2907, 2023.
- [33] M. Zipfl and J. M. Zöllner, "Towards traffic scene description: The semantic scene graph," in *25th International Conference on Intelligent Transportation Systems (ITSC)*. IEEE, 2022, pp. 3748–3755.
- [34] L. Mlodzian, Z. Sun, H. Berkemeyer, S. Monka, Z. Wang, S. Dietze, L. Halilaj, and J. Luetttin, "nusscenes knowledge graph—a comprehensive semantic representation of traffic scenes for trajectory prediction," in *Proceedings of the IEEE/CVF International Conference on Computer Vision*, 2023, pp. 42–52.
- [35] Z. Hu, Y. Dong, K. Wang, and Y. Sun, "Heterogeneous graph transformer," in *Proceedings of the Web Conference*, 2020, pp. 2704–2710.
- [36] H. Caesar, V. Bankiti, A. H. Lang, S. Vora, V. E. Liong, Q. Xu, A. Krishnan, Y. Pan, G. Baldan, and O. Beijbom, "nusscenes: A multimodal dataset for autonomous driving," in *Proceedings of the IEEE/CVF conference on computer vision and pattern recognition*, 2020, pp. 11 621–11 631.
- [37] A. Paszke, S. Gross, F. Massa, A. Lerer, J. Bradbury, G. Chanan, T. Killeen, Z. Lin, N. Gimelshein, L. Antiga *et al.*, "Pytorch: An imperative style, high-performance deep learning library," *Advances in neural information processing systems*, vol. 32, 2019.
- [38] M. Fey and J. E. Lenssen, "Fast graph representation learning with PyTorch Geometric," in *ICLR Workshop on Representation Learning on Graphs and Manifolds*, 2019.
- [39] I. Loshchilov and F. Hutter, "Decoupled weight decay regularization," in *International Conference on Learning Representations*, 2017.
- [40] T. Phan-Minh, E. C. Grigore, F. A. Boulton, O. Beijbom, and E. M. Wolff, "Covernet: Multimodal behavior prediction using trajectory sets," in *Proceedings of the IEEE/CVF conference on computer vision and pattern recognition*, 2020, pp. 14 074–14 083.
- [41] N. Deo and M. M. Trivedi, "Trajectory forecasts in unknown environments conditioned on grid-based plans," *arXiv preprint arXiv:2001.00735*, 2020.
- [42] T. Salzmann, B. Ivanovic, P. Chakravarty, and M. Pavone, "Trajectron++: Dynamically-feasible trajectory forecasting with heterogeneous data," in *Computer Vision–ECCV: 16th European Conference, Glasgow, Proceedings, Part XVIII 16*. Springer, 2020.
- [43] R. Giris, F. Golemo, F. Codevilla, M. Weiss, J. A. D'Souza, S. E. Kahou, F. Heide, and C. Pal, "Latent variable sequential set transformers for joint multi-agent motion prediction," in *International Conference on Learning Representations, ICLR 2022*, 2022.
- [44] C. Wang, Y. Wang, M. Xu, and D. J. Crandall, "Stepwise goal-driven networks for trajectory prediction," *IEEE Robotics and Automation Letters*, vol. 7, no. 2, pp. 2716–2723, 2022.